Supporting Information

Hydrogen Bonding-Induced Hydrophobic Assembly Yields Strong Affinity of Adsorptive Membrane for Ultrafast Removal of Trace Organic Micropollutants from Water

Qilin Gui,[a] Jinxing Zhang,[a] Kexing Hu,[a] Qi Ouyang,[a] Shuxian Shi,[b] and Xiaonong Chen*[a]

[a] Beijing Laboratory of Biomedical materials, Beijing University of Chemical Technology, Beijing, 100029 P.R. China. E-mail: chenxn@mail.buct.edu.cn

[b] Key Laboratory of Carbon Fiber and Functional Polymers, Ministry of Education, Beijing University of Chemical Technology, Beijing, 100029 P.R. China.

Contents

Data for comparison in membrane adsorption performance

Adsorptive membrane, combining the advantages of adsorbent materials and separation membrane, has attracted much attention in recent years due to its large flux, low operating pressure, and low energy consumption.

Table S1. Initial concentration of pollutants investigated by adsorptive membranes

Adsorptive membrane	Model pollutant*	Initial concentration (mg/L)	Ref. /Year
Porous aromatic framework modified electrospun fiber membrane	IBPF, CLXN DEET	**50-400**	2019[1]
Macroporous membranes doped with micro-mesoporous β-cyclodextrin polymers	BPA, 2,4-DCP 2-NO, PR	**5-50**	2019[2]
Hierarchical porous membrane via electrospinning PIM-1	Carbendazim Phenol	**5-200**	2018[3]
Alkylbenzene-functionalized polypropylene nonwoven	DOP, DBP	**10-110**	2018[4]
Electrospun nylon 6,6 membrane	BPA	**20-100**	2017[5]
HAP membranes	BPS, BPA 1-NA, 2-NO 2,4-DCP	**1-10**	2017[6]
Self-assembled porous microspheres-fibers	BPA	**10-100**	2016[7]
Cotton fabric functionalized with a β-cyclodextrin polymer	BPA	**22.8-228**	2016[8]
Amphiphilic segments on polypropylene nonwoven surface	BPA, DBP DMP, DOP	**5-100**	2015[9]
Modified polypropylene fiber stacked membrane (MPPM)	BPA, BPS 2-NO, 2,4-DCP PR	**0.01**	**this work**

*Abbreviation: ibuprofen (IBPF), chloroxylenol (CLXN), *N,N*-diethylmetatoluamide (DEET), bisphenol A (BPA), bisphenol S (BPS), 1-naphthyl amine (1-NA), 2-naphthol (2-NO), 2,4-dichlorophenol (2,4-DCP), propranolol hydrochloride (PR), dibutyl phthalate (DBP), dimethyl phthalate (DMP), dioctyl phthalate (DOP).

As shown in Table S1, most of the investigation reported in the literature focus on the adsorption performance of adsorptive membranes at high concentrations of pollutants. Nevertheless, the environmentally relevant concentration of pollutants is

generally at μg/L, which is much lower than the initial concentration (mg/L) used in the references listed in Table S1. Adsorbents adsorb contaminants at high concentrations, which does not mean that they can also adsorb contaminants at trace level. Thus, we presented a new class of adsorptive membrane (MPPM) and investigated the adsorption performance for trace contaminants. Even the contaminants are present at environmentally relevant concentrations (several micrograms per liter water), the MPPM can efficiently capture OMPs from the rapid water flow across the membrane. It is worth to note that the initial concentration in our study is much lower than 1% of the initial concentration used in the literature.

Table S2. Specific surface area and adsorption effect (at environmentally relevant concentrations) of adsorbent materials reported in the literature*

Adsorbent material (abbreviation)	Specific surface area (m^2/g)	Model pollutant/ concentration (μg/L)	Removal efficiency	Typical condition	Ref. /Year
P-CDP	**263**	BPA/100 BPS/2.5	20%~40%	F, 25 mL/min	2016[10]
P-CD-P5A-P	**479**	BPA/100	87%	F, 16 mL/min	2019[11]
CD-TNF@CMC	**218**	BPA/10 BPS/10	94~97%	F, 0.2 mL/min	2019[12]
GAC-membrane	**900~1050**	BPA/10	NA	S, 48 h	2018[13]
CD-AC	**1050**	BPA/4	90~94%	F, 6 mL/min	2014[14]
GPAC	**717**	BPA/10	94%	S, 200 min	2016[15]
MPPM	**2~4**	**BPA/10** **BPS/10**	**94~99%**	**F, 40 mL/min**	**this work**

*NA: not available; F: flow-through adsorption; S: static adsorption.

As shown in Table S2, some porous materials (mainly including β-cyclodextrin polymers and functionalized activated carbon) show adsorption capacity for trace pollutants. Compared with these porous materials, MPPM is the least dependence on specific surface area and has the highest adsorption rate. Even at ultrahigh water flux (12700 L/(m^2h), 40 mL/min)), MPPM is able to reduce trace OMPs (10 μg/L) in water samples by up to 2-3 orders of magnitude, showing a great potential in fast production of high quality water and remediation of water resource. In addition, the process for making MPPM is quite simple and efficient compared with the energy-consuming,

batch-uncontrollable and complicated procedure for preparation of porous materials. Furthermore, it is expected that the adsorption performance of the adsorptive membrane can be significantly further promoted by replacing currently used micron-polypropylene fiber membrane with electrospinning nano-polypropylene fiber membrane as a new substrate, since the latter can provide much larger specific surface area.

1. Materials and Instrumentation

Materials: *N*-vinylformamide (NVF, Aladdin) were purified by distillation under reduced pressure prior to use and stored at -20 °C. Other chemicals were used as received, unless otherwise stated. Benzophenone (BP, Sigma Aldrich) was used as the photoinitiator. Bisphenol A (BPA, Aladdin), bisphenol S (BPS, Aladdin), 2,4-dichlorophenol (2,4-DCP, Aladdin), 2-naphthol (2-NO, Heowns), 1-naphthyl amine (1-NA, Heowns) and propranolol (PR, Heowns) tested in removal studies are representative of different kinds of organic micropollutants (OMPs). *N*-vinylpyrrolidone (NVP, Aladdin), acrylamide (AM, Aladdin), and butyl acrylate (BA, Aladdin) were used as functional monomers. All rinsing reagents, such as methanol, are HPLC grade and must be degassed before use. Ultrapure water was used to prepare various solutions.

Polypropylene fiber membranes (PPM, diameter 25 mm, equivalent pore size 5 μm), polytetrafluoroethylene membranes (PTFE), polyamide membranes (PA), polyethersulfone membranes (PES), and transparent biaxially oriented polypropylene thin-film (BOPP) were purchased from Beihua liming (Beijing, China) and used as received. Diameters and equivalent pore sizes of PTFE, PA, and PES are 50 mm and 5 μm, respectively. Other commonly used solvents were mainly purchased from Beijing Chemical Works and used without further purification.

The original PPM is polypropylene fiber (with a dimeter of about 2.2 μm) stacked membrane, similar to non-woven fabrics. The specific surface area of PPM is about 2.3

m^2/g (by BET). The apparent density is about 0.3 g/cm^3. For modified PPM with 32% grafting amount of PNVF (MPPM), the apparent density it is about 0.4 g/cm^3 and the grafting mass is about 139 mg/m^2 (coverage). The configuration of MPPM should be hairy grafts under wet condition and mushroom-like under dry condition due to aggregation of the PNVF grafts upon drying.

Instrumentation

Attenuated total reflection infrared spectra (ATR-FTIR, Nicolet 6700, USA) was used to recorded the IR spectra at room temperature. The transmitted infrared spectra of BOPP-PNVF before and after BPA adsorption at different temperatures (from 30 ℃ to 120 ℃) were recorded using a Nicolet 6700 FT-IR instrument equipped with a TGS detector and the variable-temperature cell equipped with CaF_2 windows. The cell temperature was stabilized for 5 min before measurements were obtained. Each spectrum was acquired in a wavenumber range from 4000 to 500 cm^{-1} at a resolution of 4 cm^{-1} for 32 scans. Differential IR Spectrum Analysis was used to obtain Figure 4c and the spectrum obtained at 120 °C has been subtracted from each spectrum obtained at other temperatures.[16]

X-ray photoelectron spectroscopy (XPS) analyses were performed a thermo VG (ESCALAB 250, Waltham, USA) with a monochromatic Al kalph 150 W source operating at 200 eV for survey and 30 eV for high resolution scans.

^{1}H-NMR and 2D-NOESY NMR measurements were carried out on an AV600 NMR spectrometer (BRUCKER, Switzerland). D_2O, D-DMSO, and D_2O/D-DMSO were used to dissolve samples as needed and the solutions were measured with tetramethylsilane (TMS) as the internal reference. Analytical details of 2D-NOESY NMR were set according to the previous report.[17]

Scanning electron microscopy (SEM) and energy dispersive spectroscopy (EDS) images of PPM before and after modification were taken by using a JSM-6700F instrument (JEOL, Japan). The images were obtained at a working distance of ~ 8 mm

and at beam voltages of 5 kV, except for EDS images (at 15 kV).

Ultraviolet-visible (UV-vis) spectra were recorded with a UV-Vis 2550 spectrophotometer (SHIMADZU, Japan).

Water contact angle measurements were conducted on a contact angle measuring instrument (OCA25, Germany). Different membranes were placed on glass slides. Contact angles at different times (50s for PPM and 5s for MPPM) could be recorded after 6 μL of water was dropped onto sample surfaces and each sample was measured at least three times.

Ultraviolet lamp (AT, USA) was used to initiate surface polymerization and the power could be adjusted from 10 to 400 W and the wavelength was 365 nm.

The fluorescence measurements were carried out on a F2500 spectrofluorometer (HITACHI, Japan). The excitation wavelength was 334 nm and the I_1/I_3 ratio was calculated as the ratio of peak I (*ca.* 374 nm) and peak III (*ca.* 385 nm) in the vibration fine structure of pyrene monomer emission.

The molecular weights of the polymer were measured using an YL9100 GPC SYSTEM (YOUNG LIN, Korea) equipped with a pump, a RI detector and a Waters Styragel HR 5E column. A set of monodisperse Polyethyleneglycol standards were used as calibration standard. Water (0.1 mol/L $NaNO_3$) was used as an eluent with a flow rate of 0.75 mL/min at 25°C.

The quantitative analysis of the removal efficiency of OMPs were performed by an upgraded HPLC (Water, USA) and AKTAprime plus (GE, USA). The detailed methods were described in section 3 (Detailed Methods and Data Analysis of Flow-through Experiments).

2. Synthetic Procedure

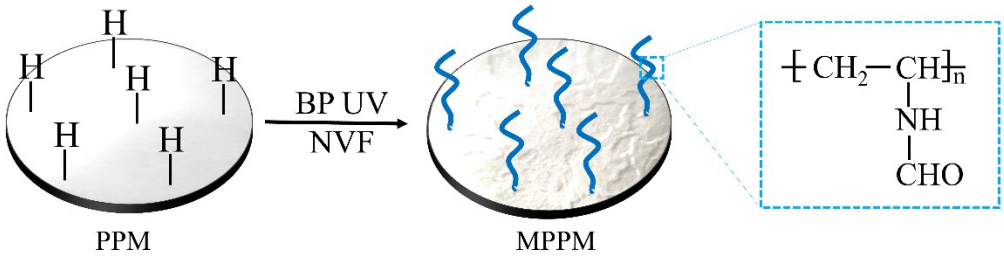

Figure S1 Schematic representation of the preparation of MPPM

The modified polypropylene fiber membranes were prepared by one-step UV grafting. In a typical example, NVF (1.60 g, 20%) was dissolved in 3.65 g water and BP (0.32 g, 4%) was dissolved in 2.45 g acetone, and then they were mixed to obtain the reaction solution. The membrane was placed in a circular groove in the center of the two quartz plates and 0.3 mL of the reaction solution was added. Subsequently, the equipment was placed under UV light for 7.5-8.5 minutes. MPPM with a mass graft ratio of 32.2% was obtained after washing (acetone and water repeated washing, three times to remove any non-grafted polymer) and drying (60 ℃, 12 h). The washing solution was collected and subjected to GPC measurement to obtain the molecular weight of the polymer generated during UV initiated polymerization, which could be used to approximately assessment of the molecular weight of the polymer grafted on the membrane surface and was found to be around 30~70 kDalton. A modified BOPP grafted with 32% PNVF (BOPP-PNVF) was prepared by a similar experimental process. A modified PPM grafted with 16% PNVF (MPPM-16%) was prepared using the above method, except that the NVF concentration was reduced to 7.5%. Note that, the weight grafting rate could be adjustable by changing the reaction conditions such as NVF concentration, illumination time, light intensity etc. The weight graft ratio was calculated by the following formula:

$$G = \frac{m_1 - m_0}{m_0} \times 100\% \quad (1)$$

where G is the weight graft ratio; m_0 and m_1 are the weights of the membrane before

and after grafting, respectively.

3. Methods and Data Analysis

Methods: All flow-through experiments were performed on the upgraded HPLC and AKTAprime plus, unless otherwise specified. A membrane cell (diameter 20 mm) was used to replace the C18 column and the concentration of the solution flowing-through the membrane cell could be acquired online in real time. The experiment process was shown in the figure below (Figure S2). The membrane cell was filled with 10 layers of test membranes (*ca.* 0.2 g, 0.5 cm^3, stacking thickness is about 1.5 mm). There are two modes: batch injection mode and continuous injection mode. Batch injection mode was usually used for flow-through experiments at high concentrations. The injection volume could be determined by different size sample loops, such as 20 μL, 0.5 mL, 2 mL, 5 mL, etc. Generally, we chose 20 μL for HPLC and 0.5 mL or 5 mL for AKTAprime plus.

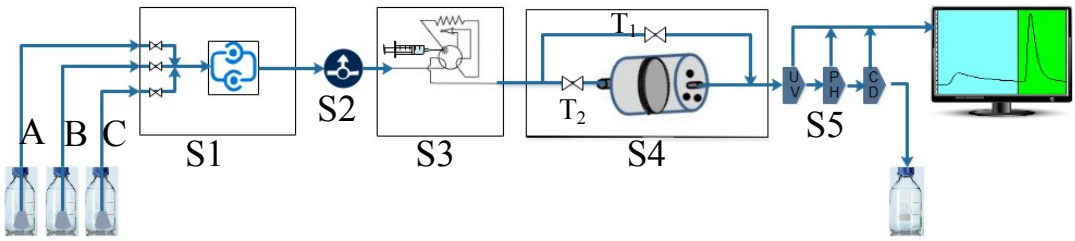

Figure S2. Process diagram of the flow-through experiments. A, B and C represent three mobile phases; S1~S5 represent flow rate control system, pressure sensor, injection system, membrane cell and detection system, respectively. T_1, T_2 represent two manual switches for connecting/unconnecting the membrane cell.

Condition for high concentration flow-through experiments: first, balance the baseline with phase A (water); second, inject the sample and begin recording the concentration of the flow-through solution; third, after the flow-through peak appeared, switch to elution phase B (ethanol, methanol, aqueous sodium hydroxide or their mixture) at 10 minutes to obtain the elution peak. The flow rate is 1 mL/min, unless otherwise stated. Each baseline is recorded using the same conditions except that no

sample is injected.

Condition for trace concentration flow-through experiments: first, balance the baseline with phase A (water); second, switch to phase C to continuously inject the trace contaminants solution (10 μg/L) for 200 mL (BPS, 2-NO) or 400 mL (BPA, 1-NA, 2,4-DCP and PR) at a flow rate of 4 mL/min (ca. 1270 L/(m^2h)); third, adjust the flow rate to 1 mL/min and switch to phase A and begin recording the concentration of the flow-through solution; fourth, switch to elution phase B at 10 minutes to obtain the elution peak. Each baseline is recorded using the same conditions except that no sample is injected.

Condition for standard sample flow-through experiments: first, balance the baseline with elution phase B; second, inject the sample and begin recording the concentration of the flow-through solution to obtain the adsorption curve. The flow rate is 1 mL/min.

Condition for static adsorption experiments: adsorptive membrane, 5 layers (*ca.* 0.16 g), BPA 200 mg/L 40 mL, 5 °C, pH 7, 18 h.

Data Analysis: A typical flow-through experiment should have two independent peaks, namely the flow-through peak and the elution peak, and the elution peak appears after the flow-through peak because the elution peak could only appear after switching to the elution phase (phase B). At high concentrations, the flow-through peak may not be detected when the residual solution concentration after flowing through the membrane cell is below the detection limit, which means that almost all of the contaminants are adsorbed by the membranes. While, the elution peak may be small due to the low adsorption capacity. Therefore, the smaller the flow-through area, the larger the elution peak area, indicating that the adsorption capacity is larger. Here, the removal efficiency (R) and the apparent removal efficiency (AR) are used to quantitatively describe the adsorption performance, which can be calculated by Equations 2 and 3, respectively.

$$R = \frac{S_e}{S_{std}} \times 100\% \quad (2)$$

$$AR = \frac{S_e}{S_e + S_t} \times 100\% \quad (3)$$

Where S_e, S_t and S_{std} are the elution peak area, the flow-through peak area, and the standard peak area (the same equivalent). For more accurate results, the baseline for each eluent has been subtracted from the sample curve (for HPLC only). The error bars are usually obtained by repeated experiments, but when the results of the repeated experiments are the same, the systematic error of the instruments is used to instead.

For static adsorption experiments, the BPA uptake per unit membrane mass (Q_m) and per unit PNVF mass (Q_p) can be calculated by Equations 4 and 5, respectively:

$$Q_m = \frac{(C_o - C_e) \times V}{m_m} \quad (4)$$

$$Q_p = \frac{(C_o - C_e) \times V}{m_p} \quad (5)$$

where C_o and C_e are the BPA concentrations in the solution before and after adsorption, respectively, V is the volume of the solution, and m_m and m_p are the weight of the membrane and the polymer grafted on the PPM, respectively.

The water flux of different membranes is calculated by Equation 6:

$$J = \frac{V}{T \times A} \quad (6)$$

where J is the membrane flux (L/(m^2h)), A is the effective area of the membrane (m^2), V and T are the volume (L) and time (h) of water flowing through the membrane, respectively. Note that, in this article, both PPM and MPPM are stacked with 10 layers of membrane, and stacking thickness is about 1.5 mm. The effective diameter of the membrane is 15.5 mm.

4. Characterization of MPPM using XPS, SEM and SEM-EDS

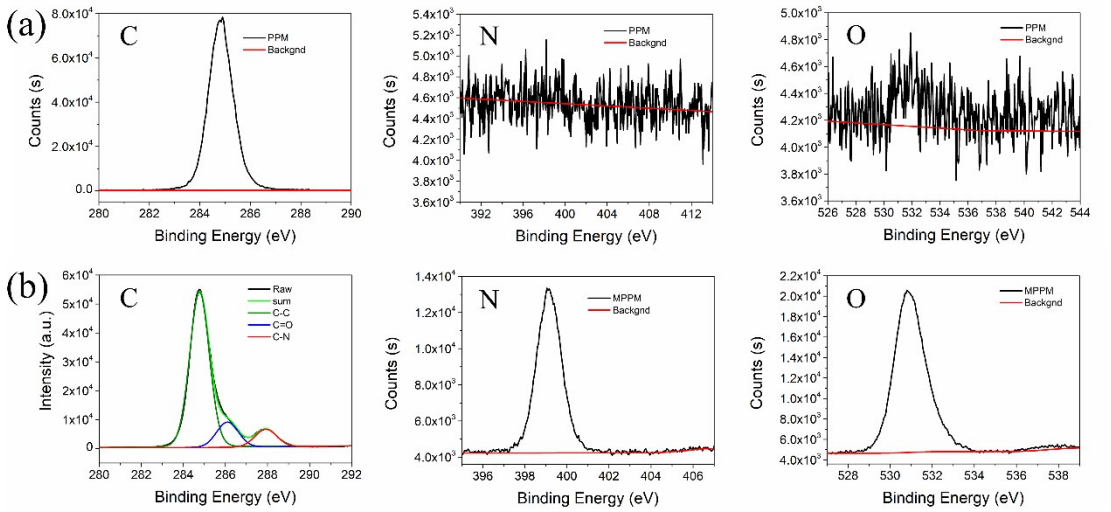

Figure S3. XPS of PPM (a) and MPPM (b)

Table S3. Surface elemental content of PPM and MPPM

Sample	Element (atom %)		
	C	N	O
PPM	100	0	0
MPPM	92.2	3.7	4.1

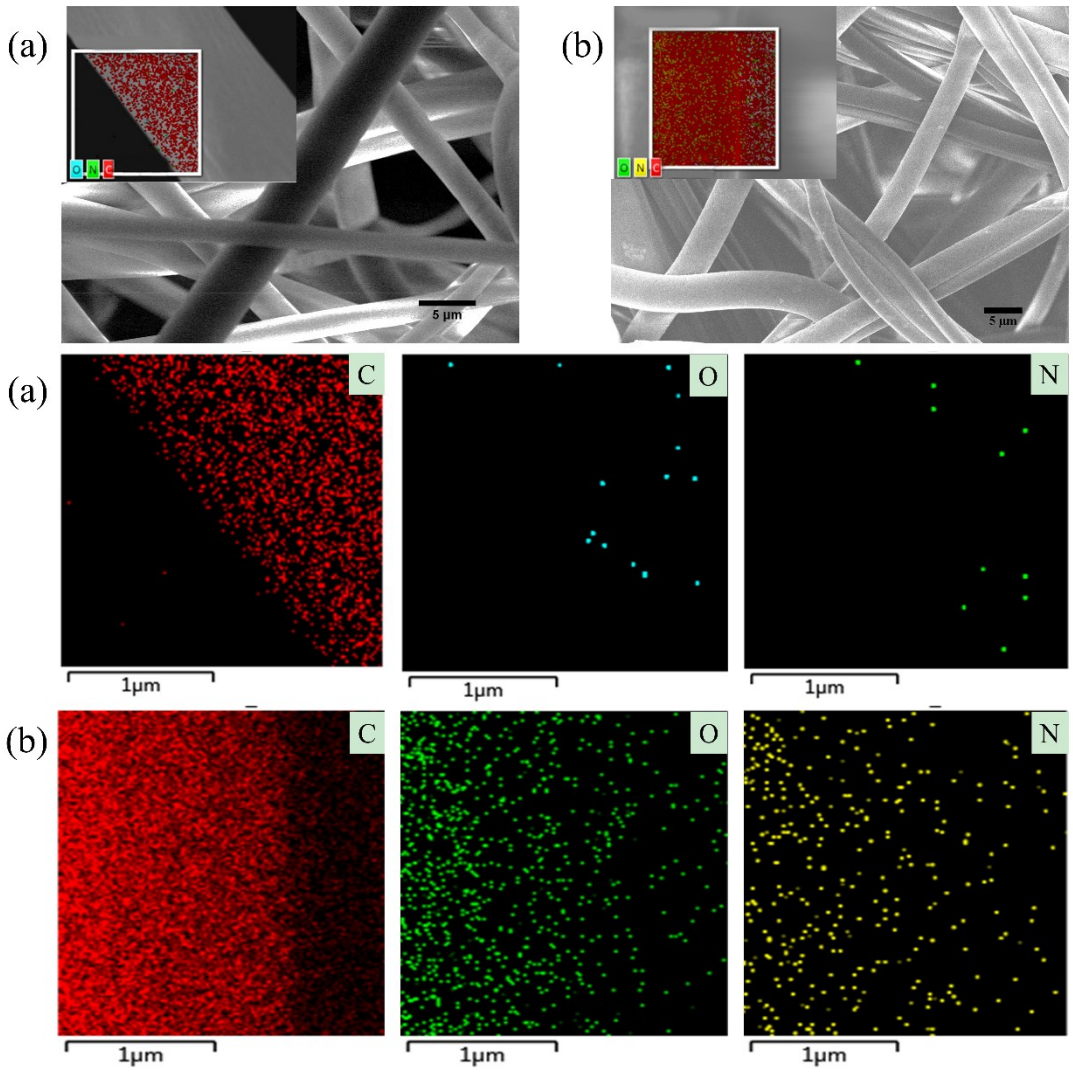

Figure S4. SEM images and EDS images of PPM (a) and MPPM (b)

5. Adsorption Property of MPPM

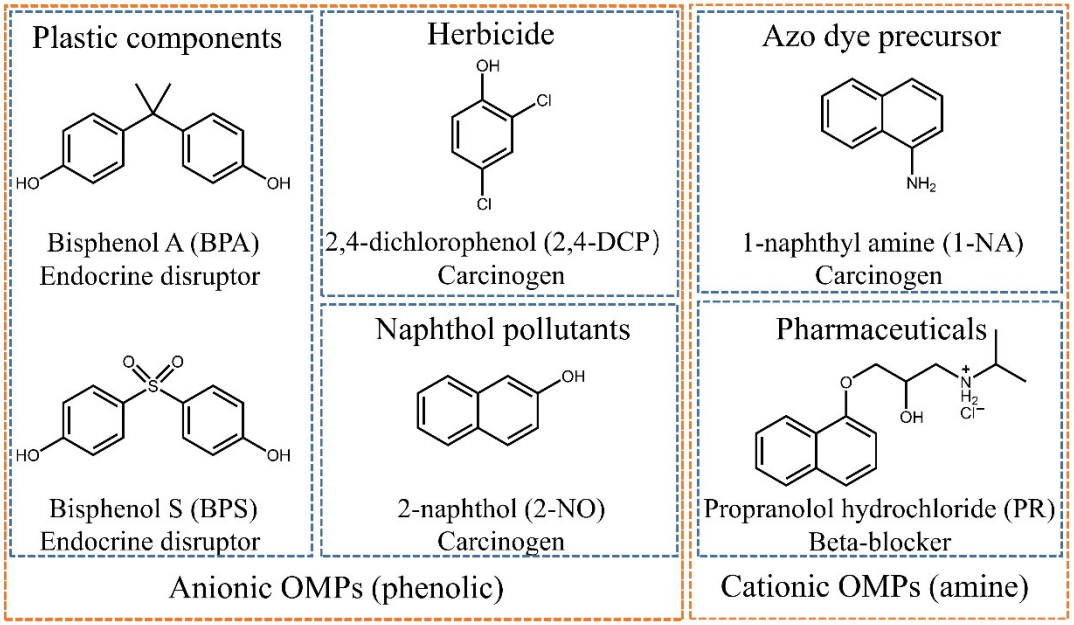

Figure S5. Structures and relevance of each tested emerging organic micropollutant.

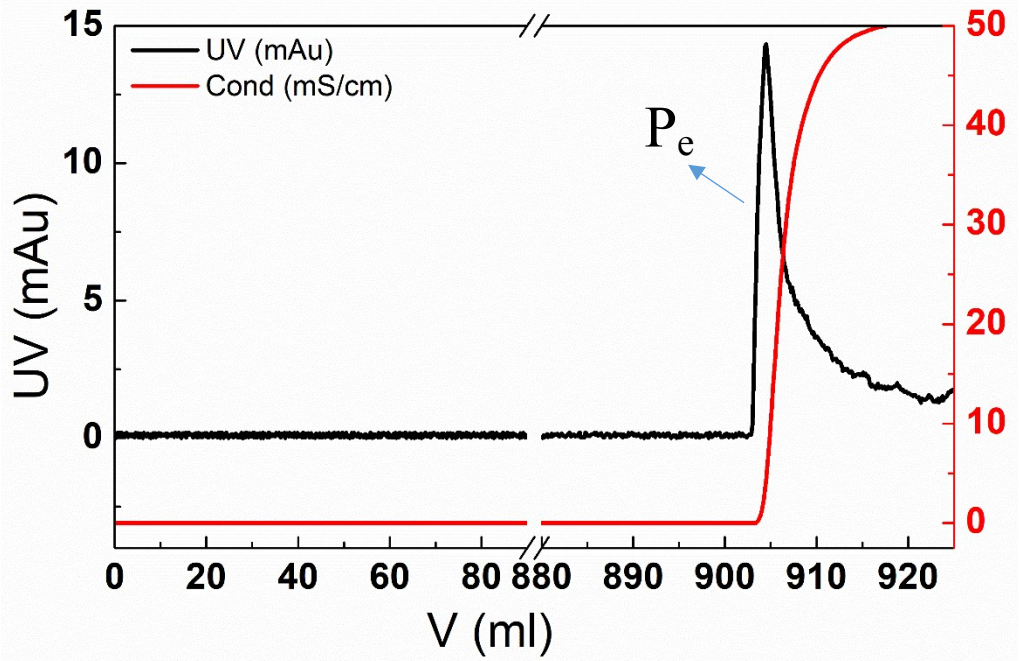

Figure S6a. Adsorbing-eluting curves of BPA at trace concentrations using MPPM as adsorptive membrane. BPA 10 μg/L, flow through 900 mL, flow rate 4 mL/min for adsorption and 1 mL/min for elution, NaOH (0.1 mol/L) elution.

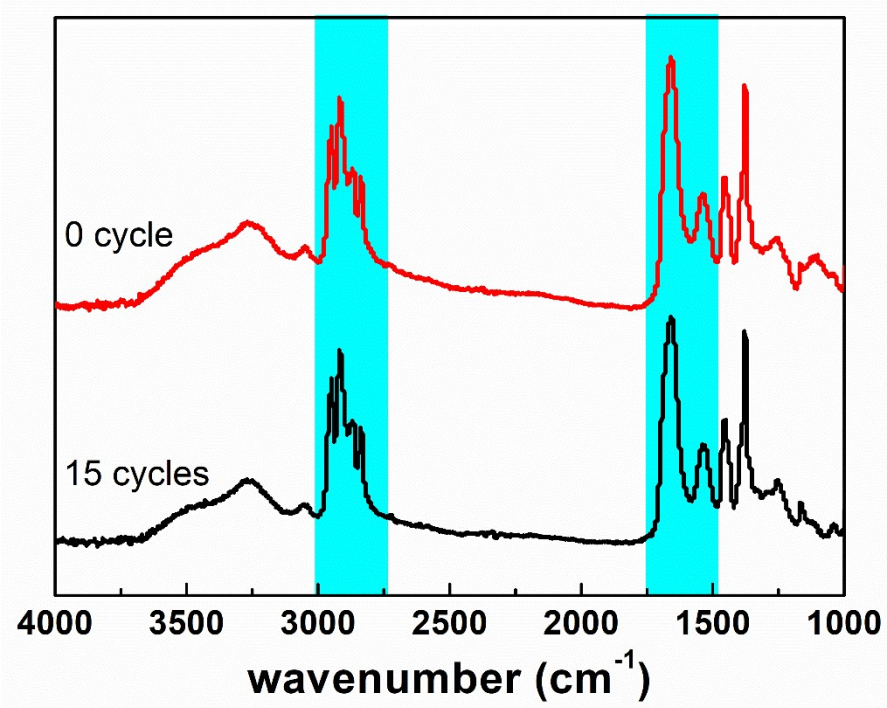

Figure S6b. FTIR spectra of the MPPM before and after 15 cycles of BPA adsorption/desorption (BPA 100 mg/L, inject 0.5 mL).

Table S4. Solute concentrating ratio of elution phase

Solute	**Flow through volume of inlet solution[1] (V_0, mL)**	**Eluent volume collected (V_e, mL)**	**Recovery efficiency (R_e, %)**	**Concentrating ratio (R_c) [2]**
BPA	900	5.5	91.4	**150**
BPA	400	2.8	92.1	**131**
BPS	400	3.5	91.5	**104**

[1] Inlet solution (adsorption phase) concentration C_0 is 10 μg/L.

[2] Concentrating ratio (R_c) is calculated as: $R_c = [C_0 \times V_0 \times R_e/V_e]/C_0 = V_0 \times R_e/V_e$.

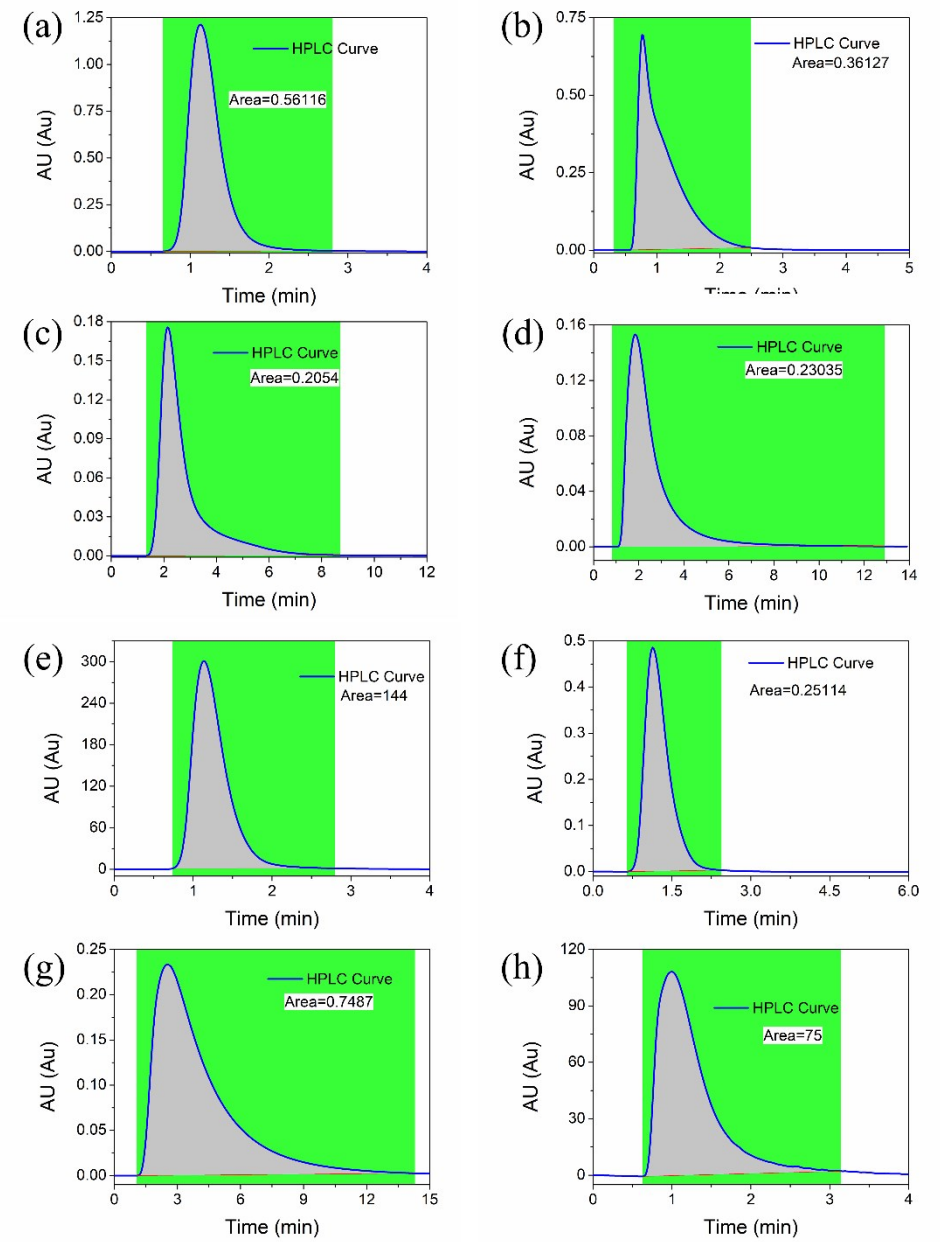

Figure S7. Real-time curves of standard samples. Flow rate, 1 mL/min; injection volume, 20μL; (a) BPA 200 mg/L, methanol elution; (b) BPA 200 mg/L, methanol/NaOH (0.1 mol/L) elution (V/V=1/3); (c) BPS 100 mg/L, methanol elution; (d) BPS 100 mg/L, methanol/NaOH (0.1 mol/L) elution (V/V=1/3); (e) 2,4-DCP 200 mg/L, methanol elution; (f) 1-NA 200 mg/L, methanol elution; (g) 2-NO 100 mg/L, methanol elution; (h) PR 200 mg/L, methanol elution.

6. Exploration of Adsorption Mechanism

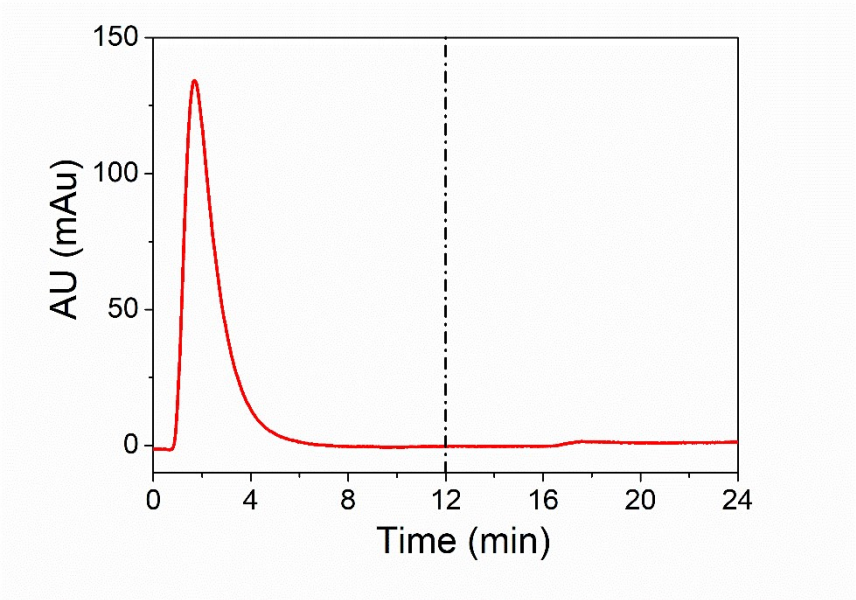

Figure S8. Adsorbing-eluting curves of hydroquinone (HQ) solution adsorbed by MPPM. MPPM 0.2 g, HQ 100 mg/L 0.5 mL, flow rate 1 mL/min. Hydroquinone (logP 1.0) is too hydrophilic to be adsorbed by MPPM, which indicates that hydrophobic interaction plays an important role in adsorption.

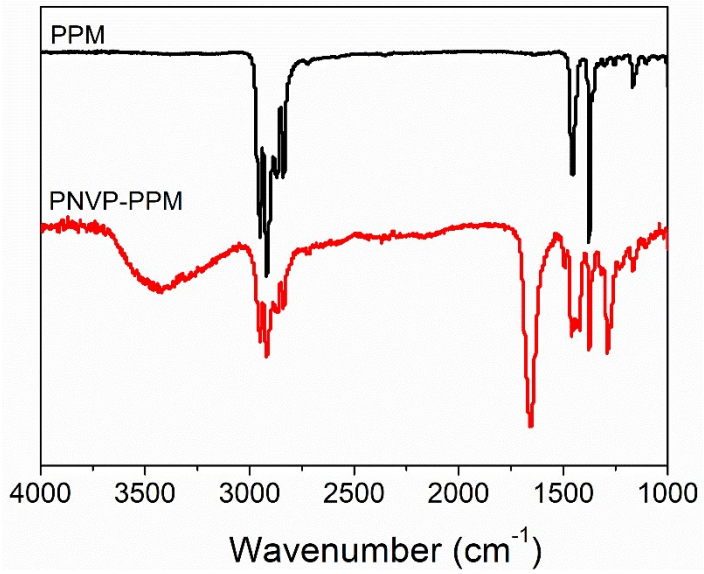

Figure S9. IR spectra of PPM (black) and PNVP-PPM (red, graft ratio 26.6%).

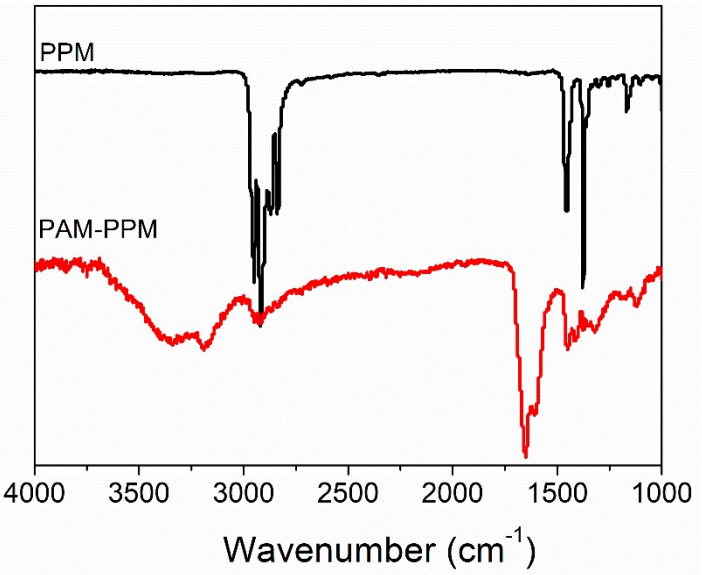

Figure S10. IR spectra of PPM (black) and PAM-PPM (red, graft ratio 29.2%).

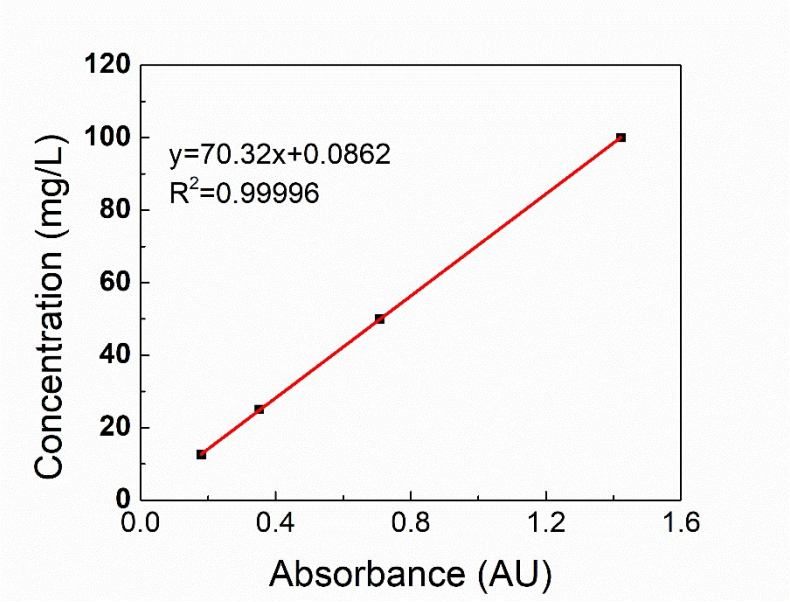

Figure S11. Calibration curve of BPA solution in water

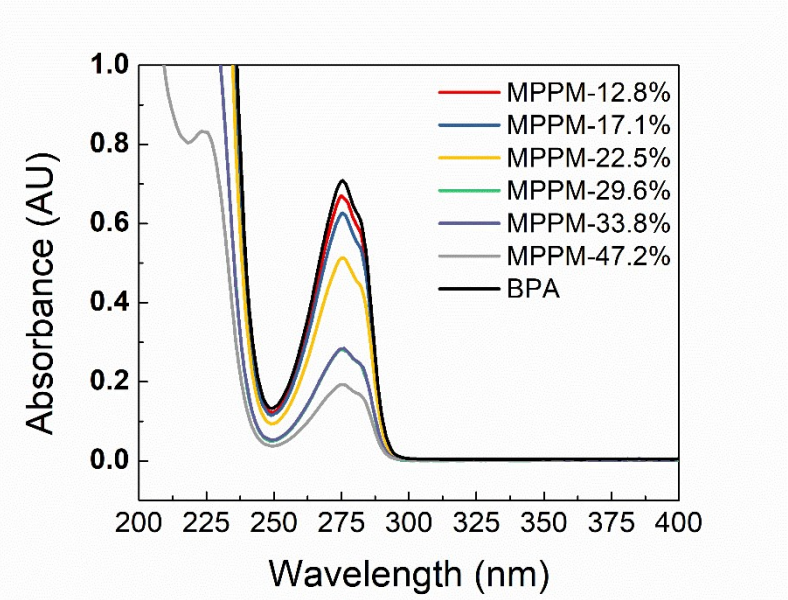

Figure S12. UV-vis spectra of BPA solution adsorbed by MPPM with different PNVF grafting ratios. BPA 200 mg/L, 40 mL, 5 °C, pH 7, 18 h. All samples were diluted 4 times for UV testing.

.

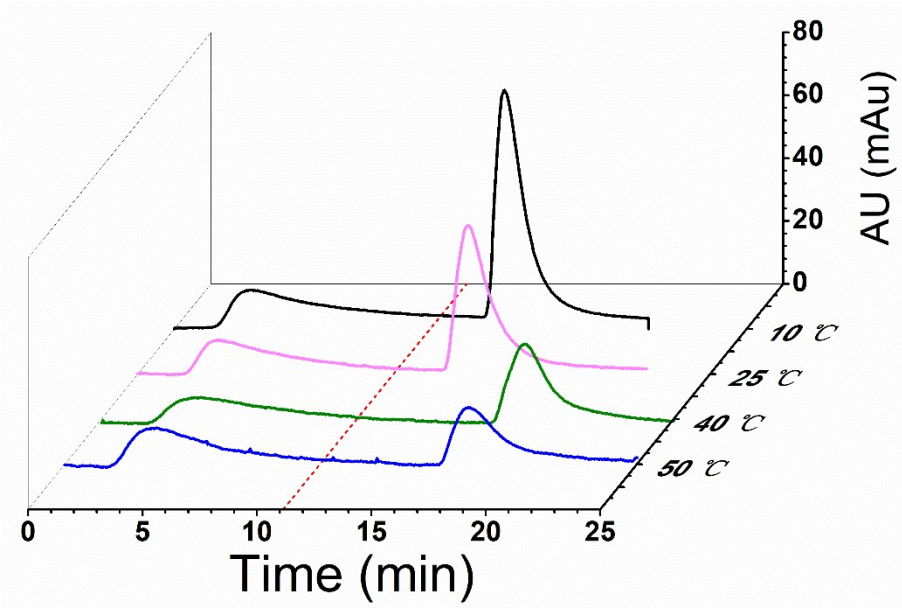

Figure S13. Adsorbing-eluting curves of BPA solution adsorbed by MPPM-16% at different temperatures. MPPM-16% 0.2 g, BPA 100 mg/L 0.5 mL, flow rate 1 mL/min.

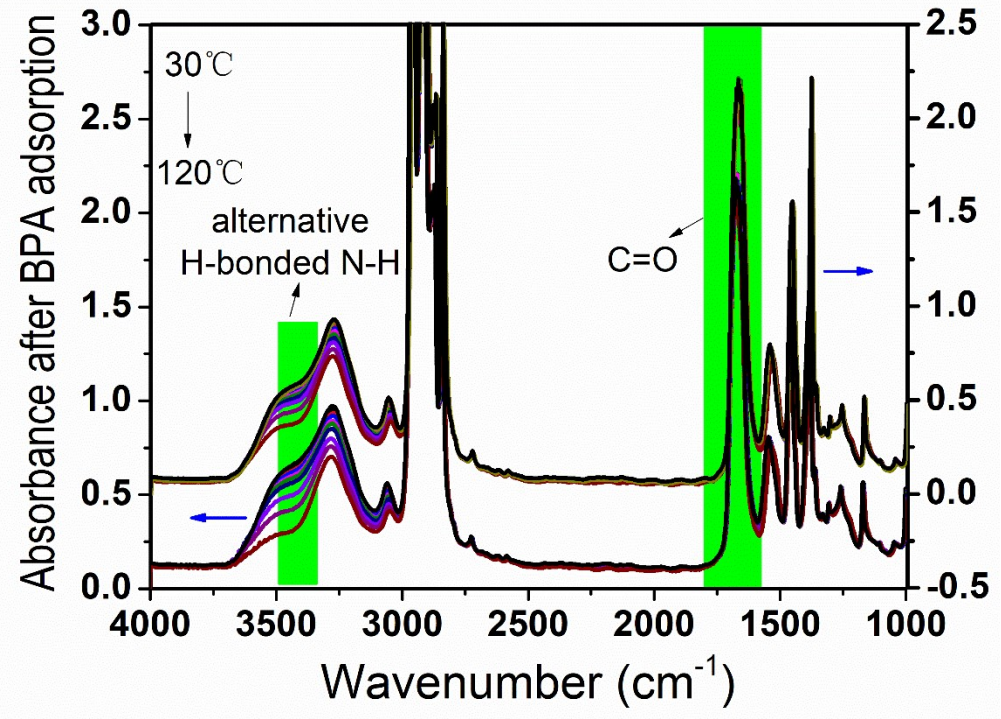

Figure S14. IR spectra (ATR) of BOPP-PNVF before and after BPA adsorption at different temperatures (from 30 °C to 120 °C). The bands centered at 3280 cm^{-1}, 3525 cm^{-1} are assigned to stable hydrogen-bonded N-H stretching signals and non- hydrogen-bonded N-H stretching signals, respectively. While the broad bands at 3370-3450 cm^{-1} are attributed to alternative hydrogen-bonded N-H stretching signals, which is much weaker than the typical amide-amide hydrogen bond.[16]

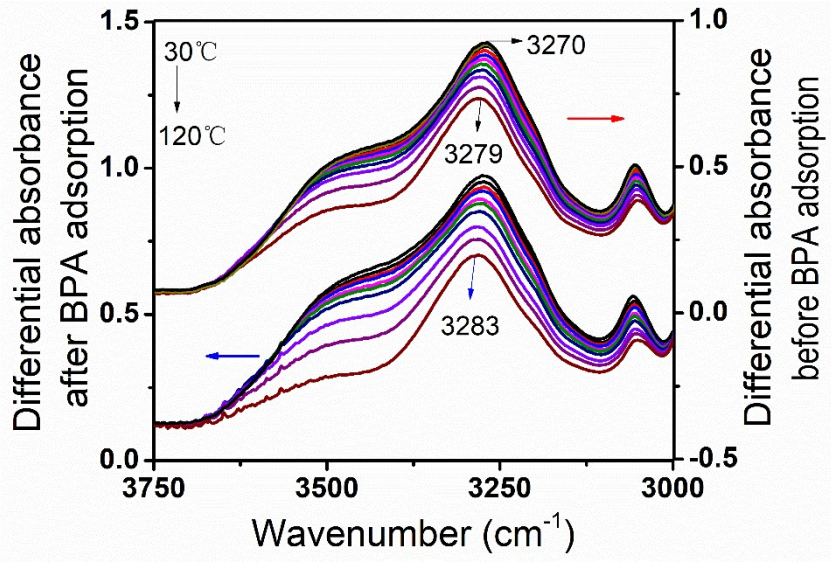

Figure S15. Differential IR spectra of BOPP-PNVF before and after BPA adsorption at different temperatures (from 30 °C to 120 °C).

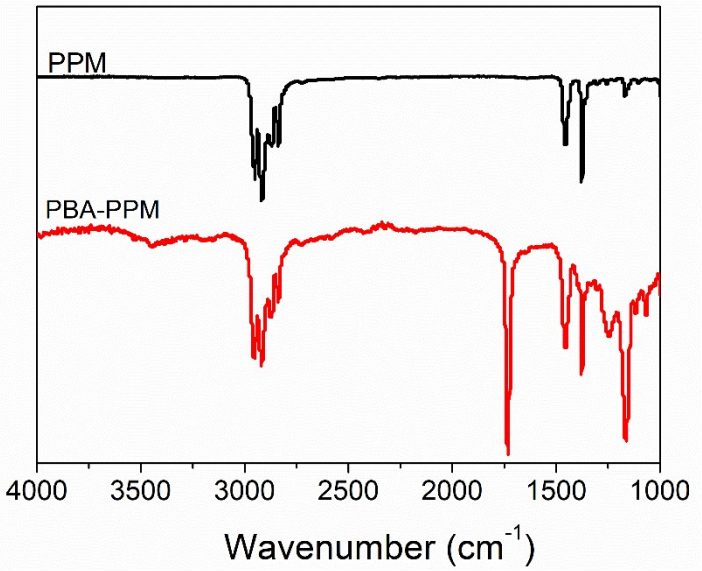

Figure S16. IR spectra of PPM (black) and PBA-PPM (red, graft ratio 28.9%).

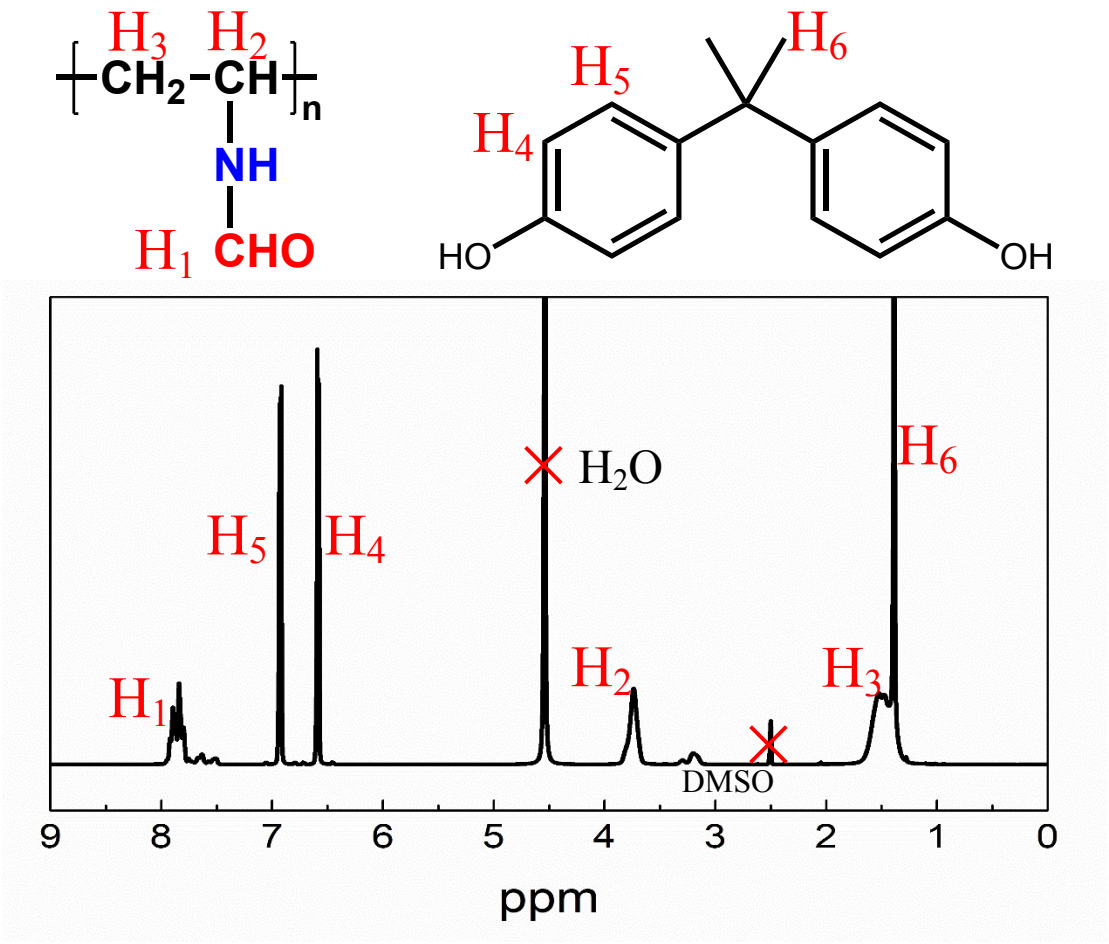

Figure S17 ^{1}H-NMR spectra for the PNVF/BPA/D_2O solutions at pH 7 (molar ratio, [BPA]/[NVF]=1:2).

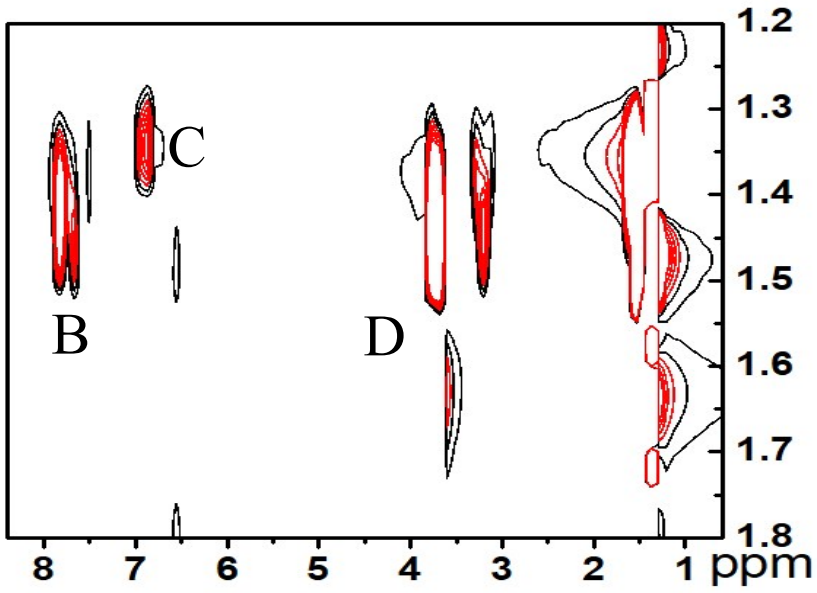

Figure S18. 2D-NOESY spectrum for the PNVF/BPA/D_2O solutions at pH 7 (molar

ratio, [BPA]/[NVF]=1:2). According to Figure S14, A was the cross peak between PNVF protons H_1 and H_2; B was the cross peak between protons H_1 (from PNVF) and H_6 (from BPA); C was the cross peak between aromatic protons H_5 (from BPA) and H_6 (from BPA); D was the cross peak between PNVF protons H_2 and H_3 (from PNVF), H_6 (from BPA).[18]

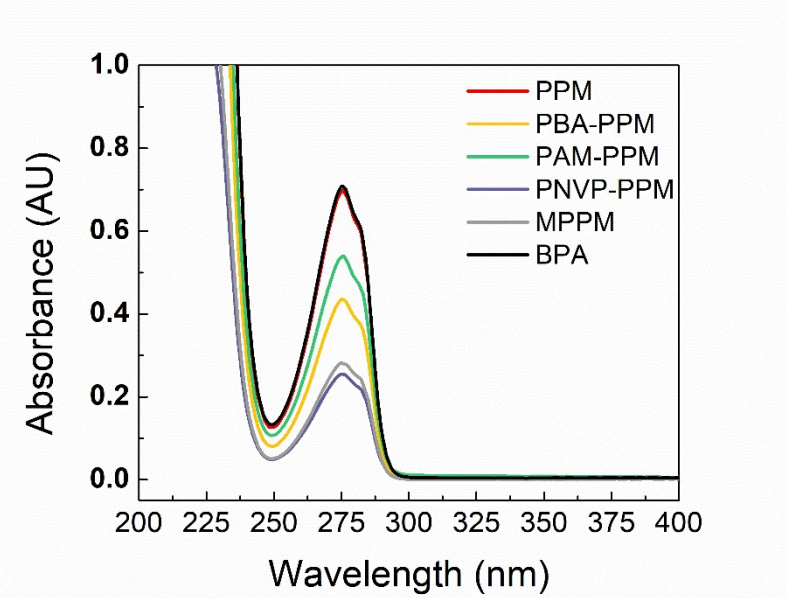

Figure S19. UV-vis spectra of BPA solution adsorbed by PPM modified with different functional polymers. BPA 200 mg/L, 40 mL, 5 °C, pH 7, 18 h. All samples were diluted 4 times for UV testing.

7. Simulating Calculation

All calculations were performed with the Gaussian program[19], and the B3LYP/6-31g(d) method was used to optimize geometric structures. The model of PNVF was composed of four monomers, and the bisphenol A (BPA) was placed on the PNVF polymer to study the interaction between them. The binding energy, E_b, of the interaction intensity between the components in the system is calculated as $E_b = \sum E_{component} - E_{total}$, where E_{total} and $E_{component}$ are the total energy of the whole system and the energy of each component in the system, respectively. Based on the above definition, a positive E_b corresponds to stable interaction between the components, and the more positive E_b indicates a stronger interaction in the system.

Table S5. Binding Energy between BPA and PNVF oligomer in different models.

Model name	Bonding type	Bonding length(Å)	Binding energy(eV)	Binding-configuration
A	O-H···O / O-H···O	1.854 / 1.794	1.33	strong+strong
B	N-H···O / N-H···O	2.256 / 2.114	0.36	weak+weak
C	O-H···O / N-H···O	1.830 / 2.063	0.62	strong+weak
D	O-H···O	1.821	0.45	strong
E	N-H···O	2.001	0.23	weak

The details geometries of these models are illustrated in Figure S20.

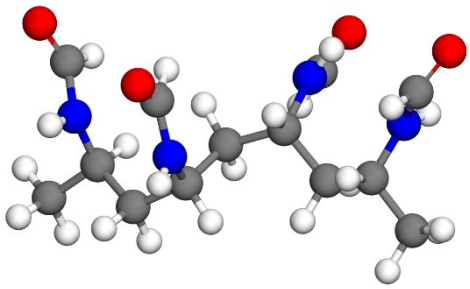

PNVF oligomer

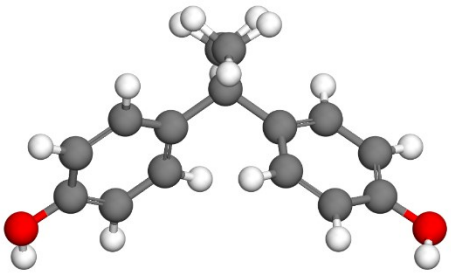

BPA

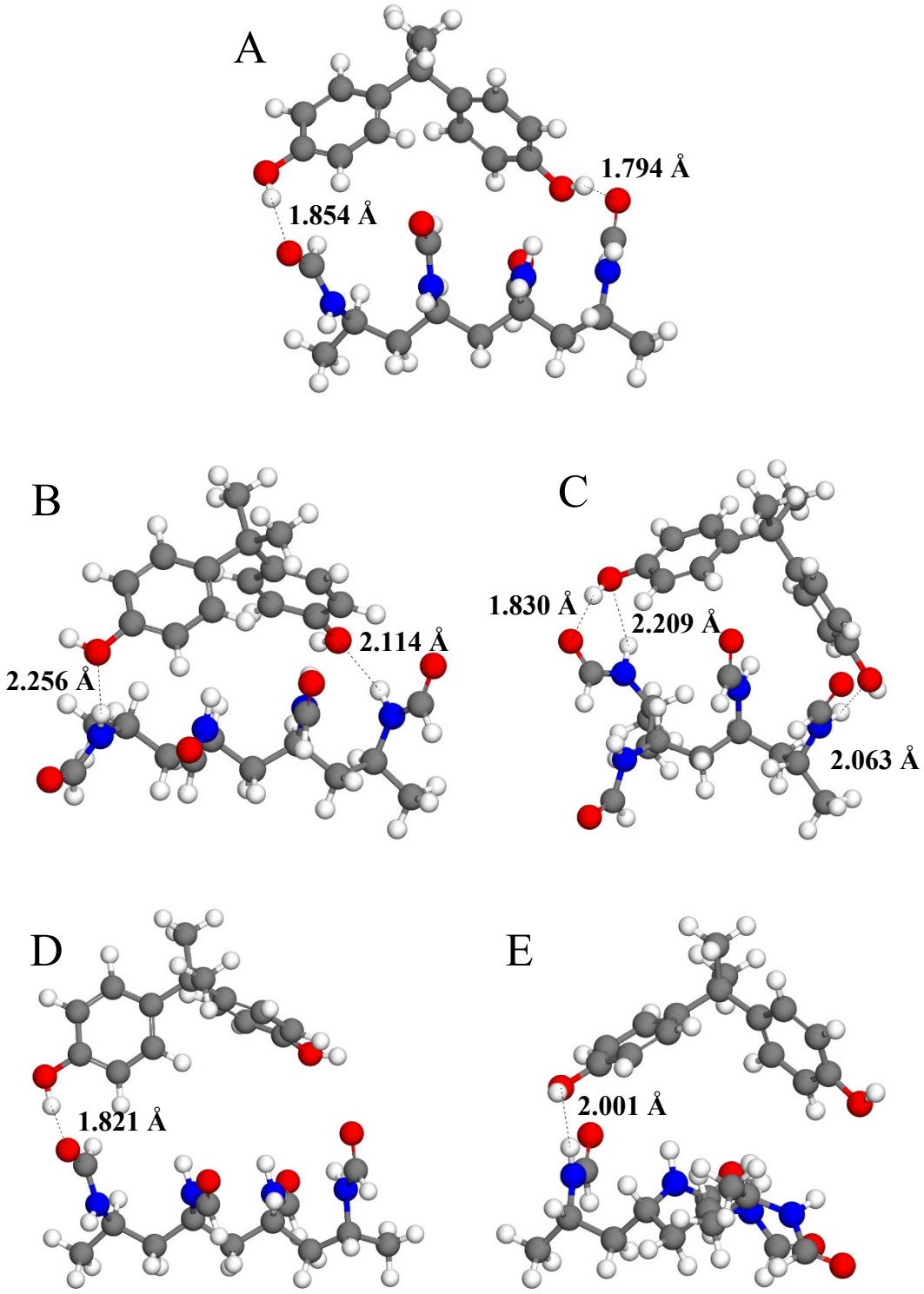

Figure S20. Proposed binding models between BPA and PNVF oligomer in different models corresponded to the entries from A to E in Table S5.

Detailed deduction of adsorption affinity[20]

Taking adsorption BPA as an example, the process of MPPM adsorption of OMPs can be simply expressed as follows:

$$BPA + MPPM = BPA_{ads} \quad (7)$$

$$k = \theta_{BPA_{ads}}/[BPA] \quad (8)$$

$$\ln k = -\Delta G/RT \quad (9)$$

$$\Delta G = \Delta H - T\Delta S \quad (10)$$

Where $\theta_{BPA_{ads}}$ is the coverage of chemically adsorbed BPA on MPPM surface, *k* is the equilibrium constant to represent surface affinity, ΔG, ΔH, ΔS, R, T are free energy change, enthalpy change, entropy change, gas constant and temperature, respectively.

At the same adsorption amounts and temperature, the entropy change and $\theta_{BPA_{ads}}$ are also the same, and *k* is inversely proportional to the concentration of BPA, which means that the larger *k*, the lower BPA adsorption concentration. While the affinity *k* depends on the reaction enthalpy change. So a discrepancy in the binding energies will bring dramatic discrimination in affinity by a factor of $\frac{k_{strong}}{k_{weak}}$, which can be calculated using equation (11).

$$\frac{k_{strong}}{k_{weak}} = \exp\left(-\frac{\Delta G_{strong} - \Delta G_{weak}}{RT}\right) = \exp(-\frac{\Delta H_{strong} - \Delta H_{weak}}{RT}) \quad (11)$$

Using these typical parameters (ΔH_{MPPM} *-128.3 kJ/mol*, ΔH_{other} *-50 kJ/mol*, *T 298.15 K* and *R 8.314 J/mol/K*):

$$\frac{k_{MPPM}}{k_{PPM}} \cong \exp\left(-\frac{\Delta H_{MPPM}}{RT}\right) \approx e^{51.8} \approx 3 \times 10^{22} \quad (12)$$

$$\frac{k_{MPPM}}{k_{other}} \cong \exp\left(-\frac{\Delta H_{MPPM} - \Delta H_{other}}{RT}\right) \approx e^{31.6} \approx 5 \times 10^{13} \quad (13)$$

The improved adsorption affinity can significantly increase the adsorption rate.

References

[1] R. Zhao, T. Ma, S. Li, Y. Tian, G. Zhu, *ACS Applied Materials & Interfaces* **2019**, *11*, 16662.

[2] Z. Wang, B. Zhang, C. Fang, Z. Liu, J. Fang, L. Zhu, *Carbohydrate Polymers* **2019**, *222*, 114970.

[3] Y. Pan, L. Zhang, Z. Li, L. Ma, Y. Zhang, J. Wang, J. Meng, *Applied Surface Science* **2018**, *443*, 441.

[4] H. Zhang, D. Fang, Z. Kong, J. Wei, X. Wu, S. Shen, W. Cui, Y. Zhu, *Chemical Engineering Journal* **2018**, *331*, 406.

[5] M. J. F. Jasni, N. A. Buang, M. Arulkumar, P. Sathishkumar, Y. A. R. Mohd, F. L. Gu, *Journal of colloid and interface science* **2017**, *508*, 591.

[6] J. He, Y. Li, X. Cai, K. Chen, H. Zheng, C. Wang, K. Zhang, D. Lin, L. Kong, J. Liu, *Chemosphere* **2017**, *174*, 380.

[7] L. Cui, J. Wei, X. Du, X. Zhou, *Industrial & Engineering Chemistry Research* **2016**, *55*, 1566.

[8] D. M. Alzate-Sánchez, B. J. Smith, A. Alsbaiee, J. P. Hinestroza, W. R. Dichtel, *Chemistry of Materials* **2016**, *28*, 8340.

[9] K. Liu, J. Wei, X. Zhou, N. Liu, *Applied Surface Science* **2015**, *337*, 178.

[10] A. Alsbaiee, B. J. Smith, L. Xiao, Y. Ling, D. E. Helbling, W. R. Dichtel, *Nature* **2016**, *529*, 190.

[11] P. Lu, J. Cheng, Y. Li, L. Li, Q. Wang, C. He, *Carbohydrate Polymers* **2019**, *216*, 149.

[12] D. M. Alzate-Sánchez, Y. Ling, C. Li, B. P. Frank, R. Bleher, D. H. Fairbrother, D. E. Helbling, W. R. Dichtel, *ACS Applied Materials & Interfaces* **2019**, *11*, 8089.

[13] L. Paredes, C. Alfonsin, T. Allegue, F. Omil, M. Carballa, *Chemical Engineering Journal* **2018**, *345*, 79.

[14] Z. M. Nagy, M. Molnár, I. Fekete-Kertész, I. Molnár-Perl, É. Fenyvesi, K. Gruiz, *Science of The Total Environment* **2014**, *485-486*, 711.

[15] J. R. Koduru, L. P. Lingamdinne, J. Singh, K. Choo, *Process Safety and Environmental Protection* **2016**, *103*, 87.

[16] S. H. Gellman, G. P. Dado, G. B. Liang, B. R. Adams, *Journal of the American Chemical Society* **1991**, *113*, 1164.

[17] R. Cong, A. D. Bain, R. Pelton, *Journal of Polymer Science Part B Polymer Physics* **2000**, *38*, 1276.

[18] J. Tzeng, S. Hou, *Macromolecules* **2008**, *41*, 1281.

[19] M. J. Frisch, G. W. Trucks, H. B. S chlegel, G. E. Scuseria, M. A. Robb, J. R. Cheeseman, G. Scalmani, V. Barone, B. Mennucci, G. A. Petersson, et al, Gaussian, Inc., Wallingford CT, 2013

[20] J. Zhou, H. Lin, X. Cheng, J. Shu, J. He, H. Li, Q. Xu, N. Li, D. Chen, J. Lu, *Materials Horizons* **2019**.